Published March 16, 2015

IgE-activated basophils regulate eosinophil tissue entry by modulating endothelial function

Laurence E. Cheng,[1,4] Brandon M. Sullivan,[2] Lizett E. Retana,[1] Christopher D.C. Allen,[3,4,5] Hong-Erh Liang,[2] and Richard M. Locksley[2,4,6,7]

[1]Department of Pediatrics, [2]Department of Medicine, [3]Department of Anatomy, [4]Sandler Asthma Basic Research Center, [5]Cardiovascular Research Institute, [6]Department of Microbiology and Immunology, and [7]Howard Hughes Medical Institute, University of California, San Francisco, San Francisco, CA 94143

Vertebrate immunity has evolved a modular architecture in response to perturbations. Allergic inflammation represents such a module, with signature features of antigen-specific IgE and tissue eosinophilia, although the cellular and molecular circuitry coupling these responses remains unclear. Here, we use genetic and imaging approaches in models of IgE-dependent eosinophilic dermatitis to demonstrate a requisite role for basophils. After antigenic inflammation, basophils initiate transmigration like other granulocytes but, upon activation via their high-affinity IgE receptor, alter their migratory kinetics to persist at the endothelium. Prolonged basophil–endothelial interactions, in part dependent on activation of focal adhesion kinases, promote delivery of basophil-derived IL-4 to the endothelium and subsequent induction of endothelial vascular cell adhesion molecule-1 (VCAM-1), which is required for eosinophil accumulation. Thus, basophils are gatekeepers that link adaptive immunity with innate effector programs by altering access to tissue sites by activation-induced interactions with the endothelium.

CORRESPONDENCE
Richard M. Locksley:
locksley@medicine.ucsf.edu

Abbreviations used: DNFB, dinitrofluorobenzene; DNP, dinitrophenol; DTA, diphtheria toxin α subunit; FAK, focal adhesion kinase; LTB4, leukotriene B4; TNP, trinitrophenol.

Inflammation comprises the immune response to infection or injury and is characterized by activation of a multistep cascade leading to the accumulation of leukocytes in involved tissues (Medzhitov, 2008). In response to a range of insults, vertebrates have evolved a "modular" immune system whereby distinct inflammatory programs are engaged depending on the nature of the perturbation. Although the cellular constituents of these inflammatory modules are largely defined, a detailed understanding of how specific modules are engaged and reinforced is lacking. Clarifying these checkpoints will enhance our understanding of immune responses in host defense and injury and across the spectrum of chronic inflammatory diseases.

Allergic inflammation is an immune module that is associated with parasitic infections and prevalent human diseases, such as asthma and atopic dermatitis. In each of these, the hallmark features of allergic inflammation include the accumulation of eosinophils in target tissues and a rise in serum antigen-specific IgE (Simon et al., 2004; Woodruff et al., 2009). Both parameters serve as biomarkers for allergic disease with the activity of IgE related to its ability to interact with high-affinity IgE receptor–bearing myeloid cells, principally mast cells and basophils. In mice and humans, Fcε receptor I (FcεRI) is constitutively expressed on mast cells and basophils, although additional cell types in humans, such as certain dendritic cells and monocytes, also express this receptor (Gould and Sutton, 2008). Mast cells and basophils derive from a common developmental precursor (Qi et al., 2013), but mature cells are anatomically separated. Basophils are rare, short-lived, blood-borne cells, whereas mast cells are long-lived, tissue-resident cells found in abundance at barrier surfaces like the skin and mucosa. Mast cells are in close proximity to blood vessels, where they can acquire serum IgE by probing the vascular space and can alter vascular function by elaboration of vasoactive mediators, such as histamine (Galli and Tsai, 2010; Cheng et al., 2013). This perivascular positioning led to the suggestion that IgE-loaded tissue mast cells released eosinophil-attracting eicosanoids and cytokines and/or promoted sensitization of

© 2015 Cheng et al. This article is distributed under the terms of an Attribution–Noncommercial–Share Alike–No Mirror Sites license for the first six months after the publication date (see http://www.rupress.org/terms). After six months it is available under a Creative Commons License (Attribution–Noncommercial–Share Alike 3.0 Unported license, as described at http://creativecommons.org/licenses/by-nc-sa/3.0/).

The Journal of Experimental Medicine

Downloaded from jem.rupress.org on March 21, 2015

The Rockefeller University Press $30.00
J. Exp. Med. 2015
www.jem.org/cgi/doi/10.1084/jem.20141671

Published March 16, 2015

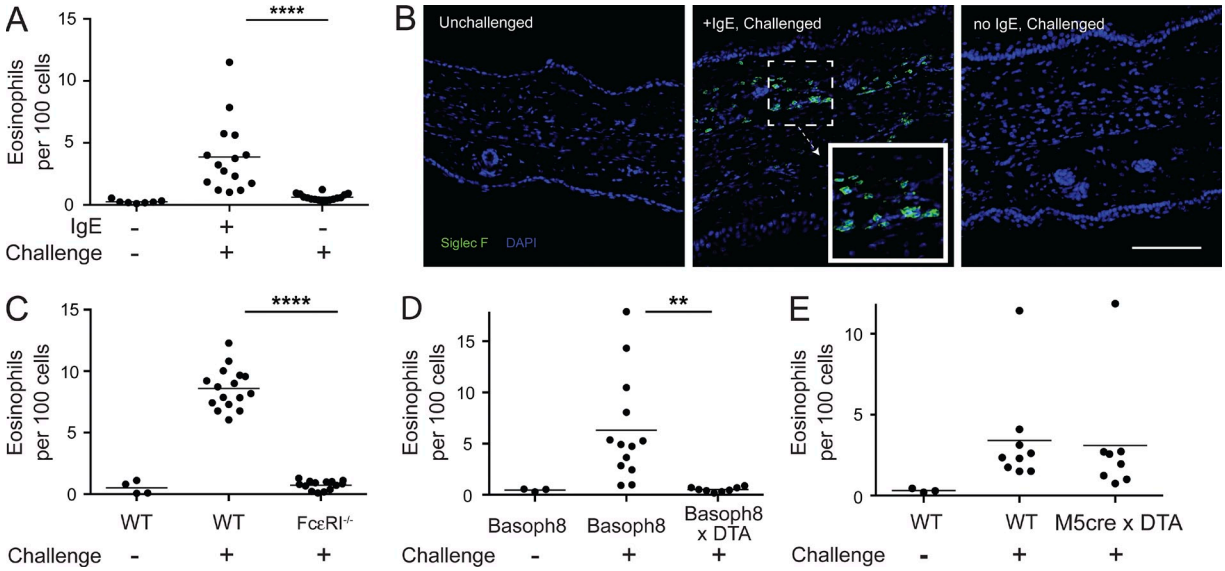

Figure 1. IgE acts as a molecular switch to drive allergic inflammation. (A) C57BL/6 mice were sensitized with anti-DNP IgE and challenged 24–36 h later with topical application of DNFB. Nonsensitized mice were used as controls. Eosinophil influx into the ear skin was measured 3 d after challenge. Results were pooled from three independent experiments with a total of at least eight mice per challenged group. (B) C57BL/6 mice were sensitized and challenged as in A, and immunofluorescence images from ears of unchallenged (left), IgE-sensitized/challenged (middle), and nonsensitized/challenged (right) mice at day 3 after challenge are shown. The inset in the middle panel depicts the staining pattern of the Siglec-F antibody and corresponds to the highlighted region. Data are representative images from two separate experiments. Bar, 100 µm. (C) FcεRIα$^{-/-}$ or WT mice bred separately were sensitized and challenged as in A, and eosinophil tissue accumulation was assessed on day 3 after challenge. Data were pooled from two separate experiments with seven to eight mice per challenged group in aggregate. (D and E) Mice constitutively deficient in basophils (Basoph8 × DTA) or mast cells (M5cre × DTA) were sensitized, challenged, and analyzed as in A. Basoph8 × DTA experiments were pooled from three separate experiments and M5cre × DTA from two separate experiments with at least eight mice per challenged group in aggregate. Basoph8 × DTA experiments were performed with littermates, whereas M5cre × DTA mice were bred distinctly from WT controls. (A and C–E) Horizontal bars denote mean. Statistical analysis was performed using ANOVA: **, $P < 0.01$; ****, $P < 0.0001$.

effector T cells in response to allergens that promoted eosinophil ingress into tissues (Liu et al., 2011). However, recent studies in a variety of models suggest an unexpected contribution of circulating basophils to allergic inflammatory responses, including the accumulation of eosinophils in target tissues (Mukai et al., 2005; Ohnmacht et al., 2010; Jin et al., 2012; Matsuoka et al., 2013). How circulating basophils influence localized eosinophil recruitment is unclear, but elucidation of this pathway could uncover new strategies for regulating allergic inflammation.

We used models of IgE-dependent eosinophilic skin inflammation that allowed us to establish the hierarchical relationships between IgE and tissue eosinophilia. Through a combination of genetic and imaging approaches, we define a role for IgE-activated basophils in regulating eosinophil accumulation. Basophils exert this effect through a three-step process. First, injury attracts rare, circulating basophils through up-regulation and activation of local vascular adhesion molecules by a process similar to that for other granulocytes. Second, activation of basophil FcεRI by antigen leads to secretion of IL-4, a necessary component of the allergic phenotype. Finally, activated basophils arrest their migration into tissues and engage in prolonged endothelial interactions, thus enabling the development of IL-4–induced endothelial vascular cell adhesion molecule-1 (VCAM-1), which is required for the arrest and recruitment of circulating eosinophils. The establishment of enhanced endothelial interactions induced by FcεRI engagement during basophil transendothelial migration into tissues explains how a rare circulating cell can establish portals of entry for eosinophils, thus uniting these canonical adaptive and innate components of allergic immunity.

RESULTS

IgE–basophil interactions act as an inflammatory switch to promote allergic inflammation

We established a model of IgE-dependent eosinophilic skin inflammation by infusing C57BL/6 mice with 2 µg dinitrophenol (DNP)-specific monoclonal IgE. After 24–36 h, by which time free IgE is cleared from the blood (Cheng et al., 2010), mice were challenged with the hapten dinitrofluorobenzene (DNFB), applied topically to the ear in a solution of acetone and dibutylphthalate, and ears were harvested for analysis at designated times. On day 3 after challenge, we observed a sixfold increase in the influx of CD11b^{+}Siglec-F^{+}Gr-1$^{lo/int}$ eosinophils only in presensitized mice (Fig. 1 A and Fig. S1). Gating of eosinophils by this strategy was further verified by expression of GFP in these cells as assessed using *4get* mice, which contain an IRES-GFP cassette immediately 3′ of the native IL-4 gene (Mohrs et al., 2001). Eosinophils, basophils, and mast cells from these mice constitutively express GFP at steady-state (Gessner et al., 2005). The data also indicated that almost all Siglec-F^{+} cells in the skin were eosinophils (Fig. S1).

Downloaded from jem.rupress.org on March 21, 2015

Published March 16, 2015

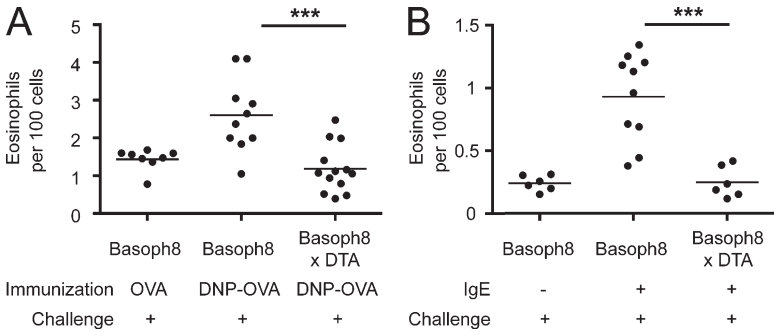

Figure 2. Basophils regulate eosinophil accumulation after vaccination and in models of human atopic dermatitis. (A) Basophil-deficient (Basoph8 × DTA) or -sufficient mice (Basoph8) were immunized with either DNP-OVA or OVA in alum and challenged with topical DNFB 10 d later. Eosinophil accumulation was examined on day 3 after challenge. Results were pooled from three separate experiments with at least eight mice per group using littermates. (B) Basophil-sufficient (Basoph8) and -deficient (Basoph8 × DTA) mice were sensitized with anti-TNP IgE through intravenous injection and challenged 1 d later by tape stripping and epicutaneous application of TNP-OVA. Eosinophil accumulation was then examined 3 d after antigen challenge. Results were pooled from two separate experiments with at least six mice per group. (A and B) Horizontal bars denote mean. P-values were determined using ANOVA: ***, $P < 0.001$.

Enumeration of eosinophils from the ear tissue of sensitized mice revealed a similar trend with a nearly fivefold increase in eosinophils as compared with unsensitized mice (not depicted). Kinetic analysis of the eosinophil response verified that day 3 was the peak of the response and that mice challenged in the absence of sensitization did not show significant accumulation of eosinophils over the same time frame (not depicted).

The differences in eosinophil infiltration were not caused by an aberrant inflammatory response because the influx of Gr-1^{hi} cells (which were mostly Ly6-G^{+} neutrophils) was similar in the presence or absence of sensitization (Fig. S1 and not depicted). Eosinophil responses were dependent on cognate antigen–antibody interactions because mice infused with OVA-specific IgE did not mount an eosinophil response (not depicted).

Although thickening of the ear tissue, consistent with inflammation, was independent of IgE sensitization, histological examination indicated that dermal infiltration by Siglec-F^{+} eosinophils required sensitization (Fig. 1 B). Whole mount confocal microscopy was used to assess the anatomical distribution of eosinophils. Eosinophils were dispersed across the skin tissue, although a "patchy" distribution was frequently noted (not depicted). Passive sensitization also led to dermal eosinophilic inflammation in Rag2$^{-/-}$ mice, confirming that innate constituents mediated the phenotype (not depicted).

The IgE-driven eosinophilic infiltration was dependent on the high-affinity IgE receptor, FcεRI, as no eosinophilic infiltration was observed in sensitized FcεRI$\alpha^{-/-}$ mice (Fig. 1 C; Dombrowicz et al., 1993). As the FcεRI is expressed primarily on mast cells and basophils in the mouse, we selectively deleted each cell line using mice expressing lineage-specific *cre* recombinase together with a cell-intrinsic *cre*-dependent deleter allele (Rosa-DTA [diphtheria toxin α subunit]). MCPT5-cre transgenic mice express *cre* from the mast cell–specific MCPT5 allele (Scholten et al., 2008), and Basoph8 mice express *cre* from the basophil-specific MCPT8 allele (Sullivan et al., 2011). Basoph8 mice contain a YFP-IRES-cre cassette replacing the first exon of *MCPT8*. Thus, Basoph8 mice promote fluorescence-based detection of basophils as well as the capacity to specifically modulate basophil number and function. When crossed to ROSA-DTA mice, MCPT5-cre and Basoph8 mice express DTA constitutively in mast cells or basophils and delete more than 95% of ear skin mast cells and 99% of circulating basophils, respectively, with no impact on the other cell population (Scholten et al., 2008; Sullivan et al., 2011); neither mouse strain alters numbers of circulating eosinophils (not depicted). After sensitization of the respective mice, eosinophil accumulation was ablated in basophil-deleted but not mast cell–deleted mice (Fig. 1, D and E).

Basophils are required for eosinophilic inflammation after active sensitization and in a mouse model of eczema

The DNFB passive sensitization system provides a system to explore the role of basophils in eosinophilic inflammation, but does not test whether basophils regulate eosinophilic inflammation in response to physiological levels of native IgE generated in response to soluble antigen. To this end, we immunized mice and tested the role of basophils in eosinophil infiltration after cutaneous antigen challenge (Fig. 2 A). Groups of basophil-sufficient and -deleter mice were immunized with DNP conjugated to OVA (DNP-OVA). The production of DNP-specific IgE was confirmed at day 8 after immunization in both strains of mice (not depicted), and at day 10, DNFB was applied to the ears. At 3 d after challenge, the Basoph8 mice immunized with DNP-OVA developed greater eosinophilic inflammation as compared with OVA-immunized controls, and as in the passive sensitization model, basophil-deleter mice had significantly decreased eosinophilic inflammation that was similar to OVA-immunized animals (Fig. 2 A).

To more closely mimic the inflammatory response observed in patients with atopic dermatitis, we examined whether basophils regulate eosinophilic infiltration after mechanical injury. Local mechanical injury in atopic dermatitis leads to the "itch–scratch" cycle in patients with atopic dermatitis and perpetuates disease activity (Boguniewicz and Leung, 2010). To induce mechanical injury, we performed tape stripping on mouse ears followed by epicutaneous application with soluble antigen in IgE-sensitized mice, in a manner akin to published protocols (Oyoshi et al., 2010). After tape stripping and antigen application, the absence of basophils significantly curtailed the magnitude of the subsequent eosinophil infiltrate

Downloaded from jem.rupress.org on March 21, 2015

Published March 16, 2015

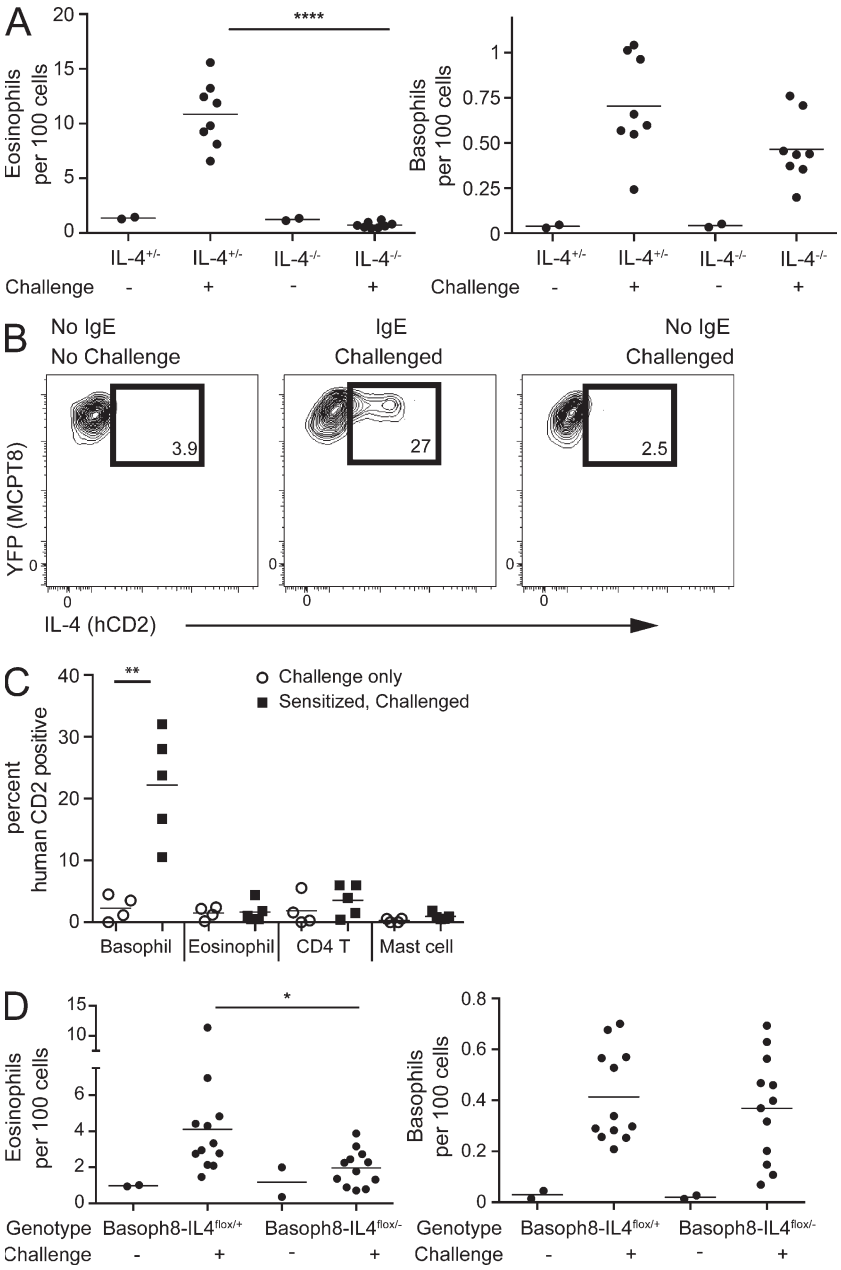

Figure 3. Basophil-derived IL-4 is required for eosinophilic inflammation. (A) IL-4$^{-/-}$ (*KN2/KN2*) and IL-4$^{+/-}$ mice on a C57BL/6 background were sensitized with anti-DNP IgE and challenged with topical application of DNFB 1 d later. 3 d after challenge, ear skin was assessed for eosinophil (left) and basophil (right) infiltration. The experiment is representative of three separate experiments with four to five mice per challenged group. The two mouse lines were bred independently to produce the indicated genotypes. (B) Basophils from Basoph8 × KN2 reporter mice were sensitized and challenged as in A. 1 d after challenge, basophils were examined for hCD2 expression at baseline (left), after IgE sensitization and challenge (middle), and after challenge alone (right). Gates were set against a KN2^{-} control sensitized and challenged in parallel. (C) Pooled results from two separate experiments performed as in A and B with four to five mice per group depicting hCD2 expression on basophils (Basoph8^{+}CD49b^{+}FSC^{lo}SSC^{lo}), eosinophils (Siglec-F^{+}CD11b^{+}FSC^{lo}SSC^{hi}), CD4 T cells (CD4^{+}FSC^{lo}SSC^{lo}), and mast cells (c-kit^{hi}CD44^{hi}CD11a^{-}, FSC^{hi}SSC^{hi}). Results from mice challenged with DNFB only (open circles) or challenge with DNFB after sensitization (closed squares) are shown. (D) Mice lacking IL-4 only in basophils (Basoph8-IL-4$^{flox/-}$) and littermate controls (Basoph8-IL-4$^{flox/+}$) were sensitized and challenged as in A. Eosinophil (left) and basophil (right) accumulation in the skin was assessed at day 3 after challenge. The data are pooled from two separate experiments with six mice per treatment group in aggregate. (A, C, and D) Horizontal bars denote mean. P-values were determined by ANOVA: *, $P < 0.05$; **, $P < 0.01$; ****, $P < 0.0001$.

(Fig. 2 B). Together, the data from these three different IgE-dependent models demonstrate that cutaneous eosinophil accumulation is controlled by basophils during both passive and active sensitization, as well as in mouse models of human atopic skin disease.

Basophil-derived IL-4 regulates eosinophil entry into the skin

Basophils produce large amounts of IL-4 after FcεRI ligation (Sullivan et al., 2011), and overexpression of IL-4 is sufficient to drive eosinophilic skin inflammation (Chan et al., 2001). Although sensitized and DNFB-challenged C57BL/6 IL-4$^{+/-}$ mice developed tissue eosinophilia comparable with wild-type mice, IL-4$^{-/-}$ mice (*KN2/KN2*) had no eosinophil accumulation (Fig. 3 A).

To examine which cells in the skin express IL-4 after sensitization and challenge, we used KN2 mice, in which a non-signaling human CD2 (hCD2) allele is targeted to the *Il4* start site, thus allowing IL-4–producing cells to be assayed directly from tissue without the need for restimulation (Sullivan et al., 2011). As noted above, this is a null *IL-4* allele. On average, nearly 25% of skin basophils from heterozygous *KN2* mice expressed the surrogate IL-4 reporter on the cell surface 1 d after challenge (Fig. 3, B and C). Moreover, hCD2 expression required prior sensitization with antigen-specific IgE. The rarity of IL-4–expressing cells precluded an unbiased assessment of IL-4 production, but direct examination of cells that can produce IL-4, including CD4^{+} T cells, eosinophils, and mast cells, revealed that none of these cell types expressed the

Downloaded from jem.rupress.org on March 21, 2015

Published March 16, 2015

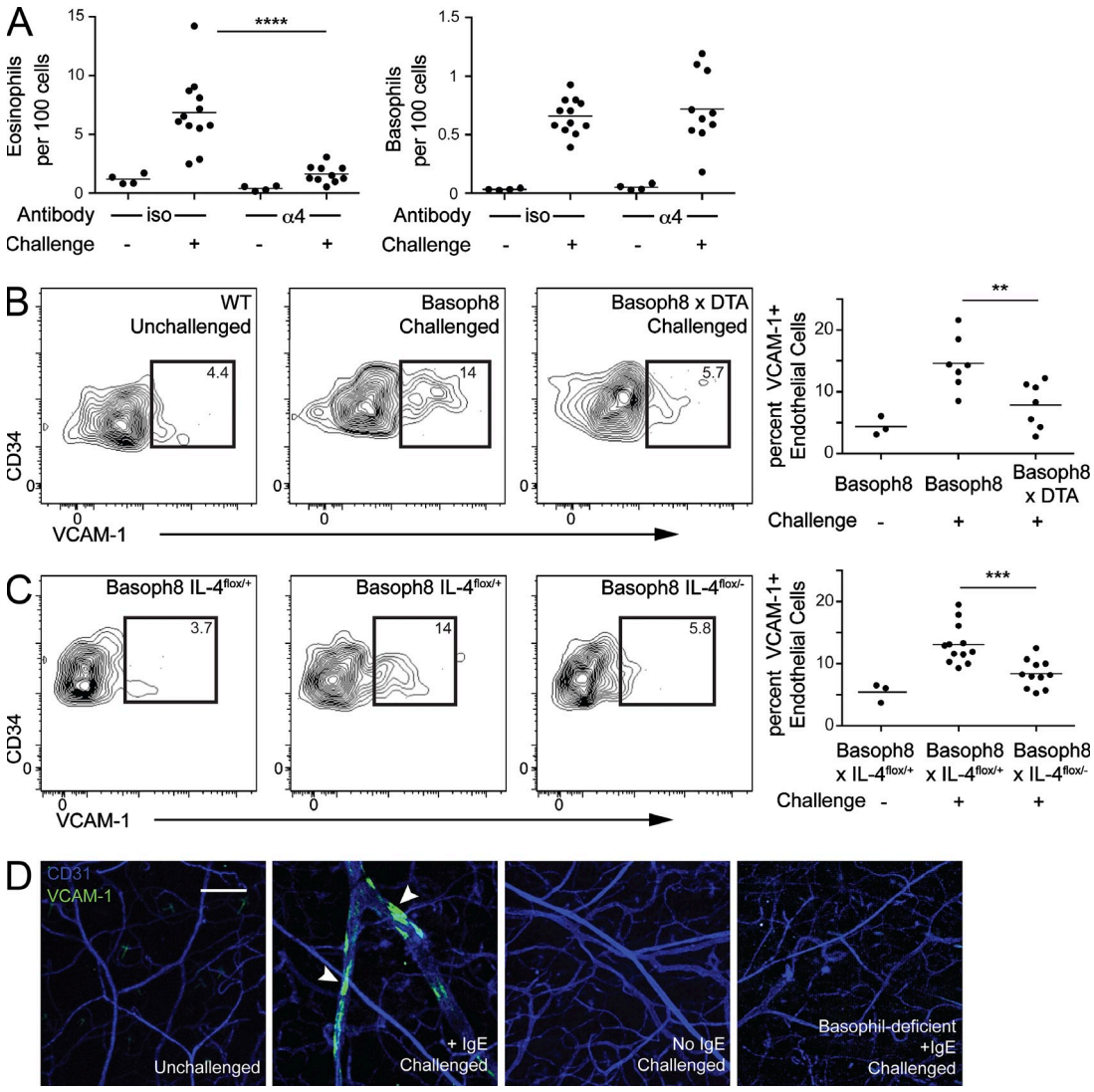

Figure 4. Basophil-derived IL-4 modulates endothelial cell expression of VCAM-1. (A) Basoph8 mice were sensitized with anti-DNP IgE, and 1 d later, the mice received anti-α4 antibody by intraperitoneal injection. Immediately after antibody administration, DNFB was applied to the ear skin of sensitized mice. Accumulation of eosinophils (left) and basophils (right) in ear skin was assessed 3 d after challenge. Results were pooled from three independent experiments with at least six mice in each challenged group. (B) Basoph8 mice were sensitized with anti-DNP IgE, and 1 d later, the mice were challenged by topical application of DNFB. 2 d after challenge, surface VCAM-1 expression on ear endothelial cells ($CD45^{-}CD34^{+}ESAM\text{-}1^{+}$) from basophil-sufficient (middle) and -deficient (right) mice was examined. The left panel depicts baseline VCAM-1 staining in unchallenged mice. Gates were set against an isotype control–stained sample. The graph on the right represents results pooled from three independent experiments with at least six mice in each challenged group. Littermate basophil-sufficient and -deficient animals were used in this experiment. (C) Basoph8 × IL-$4^{flox/+}$ (middle) and Basoph8 × IL-$4^{flox/-}$ (right) littermates were sensitized, challenged, and analyzed as in B. The contour plots are representative of the results, with the graph on the right depicting results pooled from two independent experiments with at least six mice in each challenged group. (D) WT and basophil-deficient (Basoph8 × DTA) mice were sensitized and challenged as in B. 2 d later, mice received an i.v. injection of PE-conjugated anti–VCAM-1 and APC-conjugated anti-CD31 antibody. 10 min after antibody injection, whole mount micrographs were obtained using laser-scanning confocal microscopy. Each image stack was then transformed into a maximum intensity projection with VCAM-1– and CD31-stained endothelium. The images were arranged as follows (from left to right): unchallenged WT mice, IgE-sensitized/challenged WT mice, nonsensitized/challenged WT mice, or sensitized/challenged basophil-deficient mice. Arrowheads denote VCAM-1–positive patches. The WT mice were bred independently of the basophil-deficient mice. The image is representative of two separate experiments with at least two mice in each group. Bar, 200 µm. (A–C) Horizontal bars denote mean. P-values were determined by ANOVA: **, $P < 0.01$; ***, $P < 0.001$; ****, $P < 0.0001$.

IL-4 surrogate marker (Fig. 3 C), thus identifying basophils as the primary source of IL-4 in this model. NKT cells have also been demonstrated to make IL-4, but NKT cells, as assessed by CD1d tetramer binding, were not recovered in cell populations isolated from involved ears (not depicted).

We next crossed Basoph8 mice, *KN2* mice, and *Il-4/13*$^{flox/flox}$ mice (Sullivan et al., 2011) to eliminate IL-4 specifically from basophils. *Il-4/13*$^{flox/flox}$ mice contain two loxp sites, separated by ~20 kb, that, when recombined, delete functional copies of both genes. As compared with littermate controls, mice

Downloaded from jem.rupress.org on March 21, 2015

Published March 16, 2015

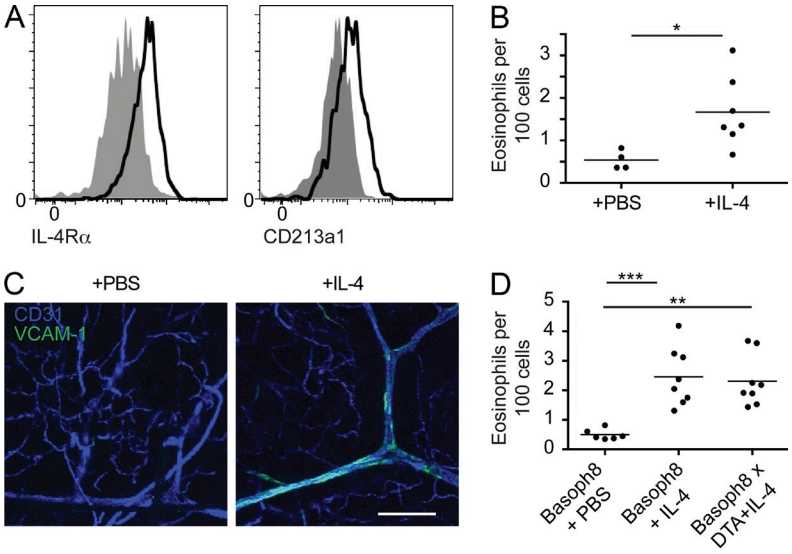

Figure 5. Endothelial cells express IL-4R and directly respond to IL-4. (A) Ear skin from WT C57BL/6 mice was homogenized, and ear skin endothelial cells ($CD45^-CD34^+ESAM\text{-}1^+$) were examined for expression of IL-4Rα (CD124) and IL-13Rα1 (CD213a1) by flow cytometry. Gray represents isotype control staining, with black lines indicative of antibody staining. Data are representative of two individual experiments with two mice examined each time. (B) C57BL/6 mice were injected with either 10 µl PBS or 100 ng IL-4 in PBS. 1 d later, eosinophil accumulation in the skin was examined by flow cytometry. Data are pooled from two separate experiments with at least four mice per group. Analysis was performed using Student's *t* test: *, $P < 0.05$. (C) C57BL/6 mice received PBS (left) or 100 ng IL-4 (right) by intradermal injection. 10 min before euthanization, the mice received i.v. anti-CD31 and anti–VCAM-1 as in B. Ear skin was then mounted and imaged using a laser-scanning confocal microscope. z-stacks were transformed into the maximum intensity projections depicted. Experiments are representative of two independent experiments with two mice per group. Bar, 150 µm. (D) Basophil-sufficient (Basoph8) or -deficient (Basoph8 × DTA) littermates were treated and analyzed as in B. Data are pooled from three separate experiments with at least six mice per group. Data were analyzed by ANOVA: **, $P < 0.01$; ***, $P < 0.001$. (B and D) Horizontal bars denote mean.

with basophil-specific deletion of IL-4 had a significant attenuation of eosinophils after challenge (Fig. 3 D). The effect was less than that observed in basophil-deleter mice or IL-4–deficient animals (Figs. 1 D and 3 A), but was consistent with the degree of cre-mediated recombination and deletion at the IL-4/13 locus (not depicted). Together, these data show that basophils are the primary source of IL-4 and that basophil IL-4 is necessary for optimal eosinophil tissue accumulation.

Basophils regulate endothelial VCAM-1

We next investigated whether IL-4 from basophils could promote eosinophil accumulation by modulating endothelial function. VCAM-1 is a STAT6-induced gene implicated in the trafficking of eosinophils to several tissues, including the skin (Tozawa et al., 2011). Antibody blockade of α4 integrin eliminated eosinophil accumulation after sensitization and challenge (Miyake et al., 1991), consistent with a role for VCAM-1 (Fig. 4 A). VCAM-1 was not required for basophil entry into the tissue, which reflects the lack of α4-integrins on mouse basophils (Voehringer et al., 2004). To assess the role of basophils in modulating endothelial VCAM-1, we analyzed VCAM-1 expression by flow cytometry on ear endothelial cells ($CD45^-CD34^+ESAM\text{-}1^+$) from sensitized ears 40 h after challenge (Baumhueter et al., 1994; Hirata et al., 2001). $VCAM\text{-}1^+$ endothelial cells were present in these mice, and expression of endothelial VCAM-1 was reduced when basophils were deleted using Basoph8 × Rosa-DTA mice (Fig. 4 B). IL-4 from basophils was required for optimal up-regulation of VCAM-1 because basophil-specific deletion of IL-4 similarly diminished VCAM-1 up-regulation on endothelial cells (Fig. 4 C). Finally, we injected anti–VCAM-1 antibody to visualize VCAM-1 on $CD31^+$ endothelial cells in situ (Fig. 4 D). Although $VCAM\text{-}1^+$ endothelial "patches" were readily apparent in sensitized and challenged mice, these patches were lost in the absence of either IgE sensitization or basophils, as assessed using Basoph8 × Rosa-DTA mice.

We verified that $CD45^-CD34^+ESAM\text{-}1^+$ skin endothelial cells uniformly express the type II IL-4 receptor, consisting of the IL-4Rα and IL-13Rα1 subunits, by flow cytometry (Fig. 5 A). We also confirmed that IL-4 alone was sufficient to mediate eosinophil accumulation and VCAM-1 expression on the endothelium by examining eosinophil accumulation in the skin after intradermal IL-4 injection (Fig. 5, B and C). Intradermal injection of IL-4 into basophil-deleter mice led to a similar degree of eosinophilic infiltration compared with wild-type mice, indicating that basophil-deleter mice have no intrinsic defect in mediating eosinophil flux into the skin (Fig. 5 D). Together, these data indicate that endothelial cells can respond to IL-4 and that IL-4 is both necessary and sufficient to mediate eosinophil skin infiltration in vivo.

Although basophil IL-4 was implicated in modulating endothelial adhesion ligands, it remained puzzling how this could be mediated by such rare numbers of circulating cells that would presumably be in relatively brief contact with endothelial cells. As assessed using direct visualization of fluorescent basophils in Basoph8 mice together with intravascular VCAM-1 labeling, basophils clustered at $VCAM^+$ endothelial patches with 2.8-fold higher density as compared with $VCAM^-$ regions (Fig. 6 A). Intriguingly, a kinetic analysis of early time points after antigen challenge revealed that accumulation of basophils in the skin of IgE-sensitized mice was delayed as compared with nonsensitized control animals (Fig. 6 B). This

Downloaded from jem.rupress.org on March 21, 2015

Published March 16, 2015

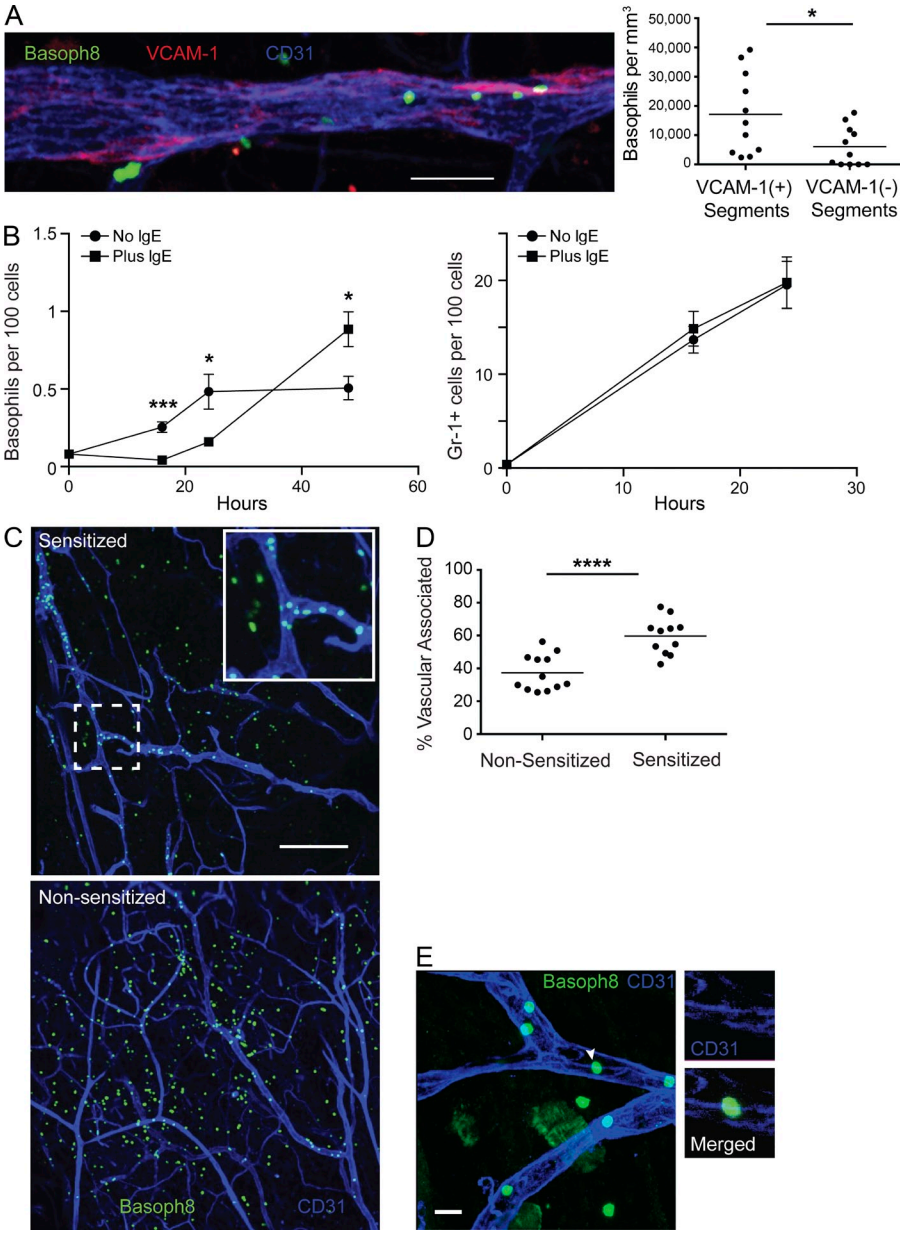

Figure 6. Activated basophils interact with the endothelium. (A, left) Basoph8 mice were sensitized with anti-DNP IgE and, 1 d later, challenged with topical application of DNFB on the ear skin. Approximately 1.5 d after challenge, the mice received conjugated anti-CD31 and anti–VCAM-1 antibody. 10 min after injection, ear skin tissue was harvested and imaged using laser-scanning confocal microscopy. A representative maximum intensity projection of basophils near VCAM-1 patches in CD31-stained endothelium from sensitized, challenged Basoph8 mice is depicted. (right) Quantification of segmented blood vessels is depicted comparing the density of basophils in VCAM-1$^+$ vessel segments with VCAM-1$^-$ segments. Each dot represents the density of basophils in segments derived from a single z-stack. Data are pooled from three mice and a total of 11 z-stacks, with a total 10-mm length of blood vessels examined with 55% of the length VCAM$^+$ and 45% VCAM$^-$. (B) Basoph8 mice were sensitized and challenged as in A with anti-DNP IgE. Basophil (left) and Gr-1$^+$ cell (right) accumulation in ear skin was then assessed at the indicated time points. IgE-sensitized mice (squares) were compared with nonsensitized mice (circles) before challenge. Error bars represent SD. Data are representative of two independent experiments with three mice at each time point. (C) Sensitized and nonsensitized Basoph8 mice were challenged with DNFB, and 24 h later, the mice received anti-CD31 conjugated to APC by i.v. injection. Mouse skin was then harvested and mounted 10 min later and imaged as in A. The images represent maximum intensity projections with basophils and CD31$^+$ blood vessels from both sensitized (top) and nonsensitized (bottom) mice. The inset depicts a zoomed-in view of the dashed box. Images are representative of three individual mice for each group with three to four z-stacks taken from each mouse. (D) The images derived from C were further analyzed for vascular-associated versus nonassociated basophils at 24 h after challenge. Each dot represents the percentage of vascular-associated basophils from a single imaging volume for the given condition. (E) Basoph8 mice were treated as in B, and a maximum intensity projection (large panel) of an ear skin whole mount from sensitized Basoph8 mice at 24 h after challenge depicting basophils associated with CD31$^+$ endothelial cell junctions is shown. The white arrowhead denotes a representative basophil associated with CD31 on the endothelium with the individual z-section and corresponding channels highlighted at the right. Image is representative of two independent experiments with at least two mice in each group. Bars: (A) 50 µm; (C) 200 µm; (E) 20 µm. (A, B, and D) Horizontal bars denote mean. P-values were derived from analysis using a two-tailed Student's *t* test: *, $P < 0.05$; ***, $P < 0.001$; ****, $P < 0.0001$.

was specific to basophils because Gr-1$^+$ cells accumulated comparably in both sensitized and nonsensitized animals over this period (Fig. 6 B).

We next performed confocal imaging of ear tissue whole mounts 24 h after challenge to assess the localization of basophils (Fig. 6 C). Basophils in nonsensitized but challenged mice were distributed widely throughout the tissues. In contrast, basophils in sensitized and challenged mice accumulated in proximity to blood vessels and were only sparsely distributed deeper in tissues (Fig. 6 C). Quantification of 2,865 basophils from nonsensitized mice and 1,494 from sensitized mice confirmed an enhanced association of basophils with the vasculature in sensitized animals (Fig. 6 D). Consistent with IL-4 being downstream of basophil clustering, we observed basophil clustering in global and basophil-specific IL-4$^{-/-}$ animals that was comparable with that in controls (not depicted). We also localized vascular-associated basophils to endothelial junctions (Fig. 6 E), which are enriched for CD31 expression and are sites for transendothelial migration

Downloaded from jem.rupress.org on March 21, 2015

Published March 16, 2015

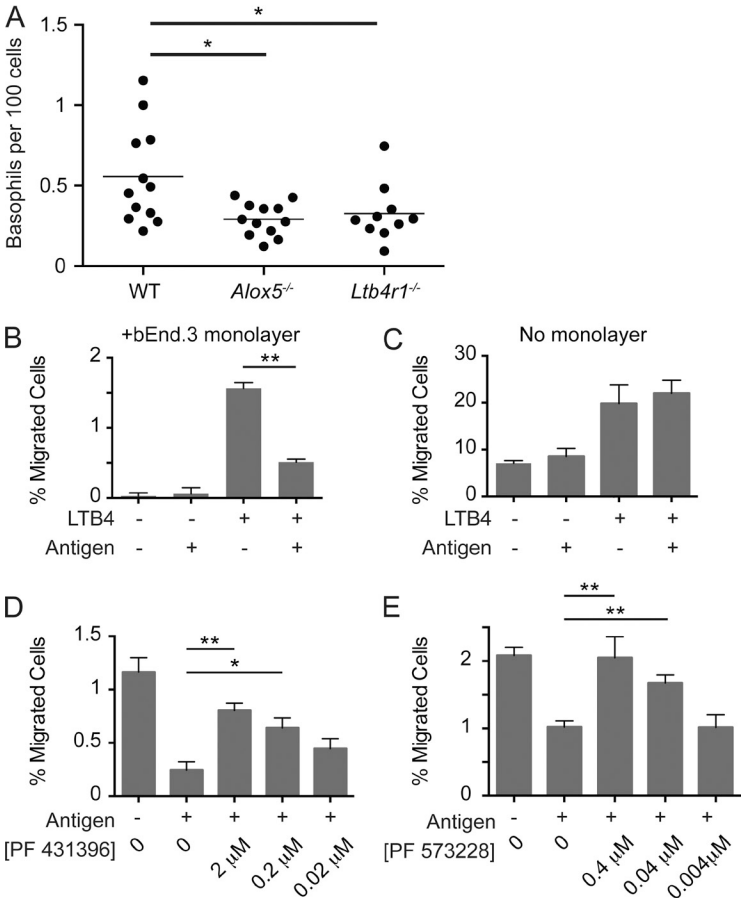

Figure 7. Basophil activation inhibits transendothelial migration. (A) WT C57BL/6, *Alox5*$^{-/-}$, or *Ltb4r1*$^{-/-}$ mice were sensitized with anti-DNP IgE and challenged with DNFB by topical application 1 d later. Basophil accumulation was analyzed 3 d after challenge. Each of these lines was bred independently, and the data were pooled from two separate experiments with at least six mice per group. Horizontal bars denote mean. (B and C) Basoph8 mice received IL-3 complex through an intravenous injection, and 3 d later, the spleens were harvested from these animals and placed in a transwell migration assay in the presence (B) or absence (C) of endothelial cells. Data are representative of four independent experiments with duplicate transwells performed each time. (D and E) Basoph8 mice were treated as in B, and the transendothelial cell migration assay was performed in the presence of the dual Pyk2/FAK inhibitor PF 431396 (D) or the selective FAK inhibitor PF 573228 (E). The concentration of each inhibitor is also noted. Data are pooled from two independent experiments each with duplicate transwells at each time point. (A–E) Student's *t* tests were performed for statistical analysis: *, $P < 0.05$; **, $P < 0.01$.

(Woodfin et al., 2011). Fully 90% of basophils ($n = 110$) were in direct contact with areas of enhanced CD31 staining. Overall, these data suggest an antigen-mediated activation event facilitates prolonged basophil interactions with the endothelium.

Basophils demonstrate activation-dependent interactions with endothelial cells

We used in vitro basophil transendothelial migration assays to explore further the nature of interactions between activated basophils and the endothelium. A prior study has demonstrated that leukotriene B4 (LTB4) acts as a migratory stimulus for basophils in vivo (Reese et al., 2007), and we confirmed that LTB4 contributes to basophil migration in our passive sensitization model using mice unable to produce (*Alox5*$^{-/-}$) or respond (*LTB4R*$^{-/-}$) to LTB4 (Fig. 7 A). Thus, we used LTB4 as a chemotactic agent for basophils expanded using IL-3 complexes in vivo and sensitized by passive transfer of anti-trinitrophenol (TNP) IgE. Basophil migration was then examined across gelatinized transwell inserts overlaid with confluent bEnd.3 endothelial cells in the presence or absence of TNP-OVA added to the bottom well to mimic the distribution of the DNFB antigen in the skin. Basophil migration across the endothelium in response to LTB4 required integrin-mediated interactions with the endothelial monolayer as antibody blockade of αL-integrin eliminated basophil migration (not depicted). Consistent with an activation-dependent interaction with the endothelium, basophil migration to the bottom well was decreased in the presence of TNP-OVA (Fig. 7 B). This decrease in migration was dependent on the presence of the endothelial monolayer because activated basophils migrated similarly in response to LTB4 in the absence of endothelial cells (Fig. 7 C). The decrease in migration caused by interactions between antigen-activated basophils and endothelial cells led us to test whether signaling pathways coincidently engaged by activated basophils and integrin-mediated adhesion altered migration kinetics. Consistent with this hypothesis, inhibition of integrin signaling with the dual focal adhesion kinase (FAK)/proline-rich tyrosine kinase 2 (Pyk2) inhibitor, PF 431396, restored basophil migration in the presence of antigen (Fig. 7 D). The effect was lost with titration of the inhibitor, and a similar increase in basophil migration was not observed in the absence of antigen stimulation at any inhibitor concentration (not depicted). Comparable experiments with a selective FAK inhibitor, PF 573228, led to a similar, albeit less pronounced, effect, suggesting that although much of the phenotype is explained by FAK inhibition, Pyk2 may also play a role (Fig. 7 E). Together, these data suggest that integration of FcεRI activation and integrin signaling arrests basophil migration, thus promoting prolonged interactions with the endothelium. Establishment of a prolonged basophil–endothelial cell interface would permit localized basophil IL-4 to induce endothelial cell VCAM-1.

Downloaded from jem.rupress.org on March 21, 2015

Published March 16, 2015

DISCUSSION

The association between eosinophilia and elevated IgE in atopy has been long known, but the mechanisms underlying this linkage have remained unclear. Using a model of IgE-dependent skin inflammation, we demonstrate that basophils enter sites of endothelial activation as with other blood-borne granulocytes but, after FcεRI ligation by antigen, alter their migratory kinetics such that prolonged interactions occur with endothelial cells. Activated basophils secrete IL-4, which induces VCAM-1 expression on the vascular endothelium necessary for entry of eosinophils, which constitutively express α4-integrins. These data reveal a novel paradigm by which rare circulating basophils can alter their migratory behavior in response to tissue-derived antigens and thereby become gatekeepers capable of changing the characteristics of the localized inflammatory response through modulation of endothelial ligands. In this way, deposition of antigen at localized sites of inflammation initiates a checkpoint that regulates subsequent eosinophil influx when basophils are labeled with antigen-specific IgE.

A study in humans and rodents over 30 yr ago linked the magnitude of eosinophil skin infiltration with the degree of basophil infiltration (Askenase, 1979). Although a causative role for basophils was speculated, this study was unable to distinguish contributions by basophils from mast cells. More recent approaches have coupled robust genetic and immunological tools that have allowed increasing resolution of the mechanisms involved in IgE-mediated allergic dermatitis. By using transgenic mice overexpressing antigen-specific IgE or passive transfer, together with antibody-mediated depletion of basophils, Mukai et al. (2005) demonstrated a requirement for basophils in IgE-mediated dermatitis. Subsequent work using genetic approaches to eliminate basophils confirmed these findings (Ohnmacht et al., 2010; Jin et al., 2012; Matsuoka et al., 2013). Although the cellular requirements for basophils in IgE-mediated allergic dermatitis became apparent, the mechanism responsible for eosinophil recruitment remained elusive. Activated basophils in skin were reported to produce IL-4 (Mukai et al., 2005), where the function was attributed to directing monocyte differentiation to alternatively activated macrophages that limited damage caused by local inflammation (Egawa et al., 2013). Our findings explain the previously unclear connection between IgE and eosinophil accumulation by linking basophil-derived IL-4 to the earliest events that dictate the hallmarks of cutaneous allergic disease.

As with other allergic diseases, including asthma and eosinophilic esophagitis, eosinophil infiltration of the skin serves as a biomarker of disease activity (Simon et al., 2004). These data suggested a key therapeutic target, but early clinical trials with anti–IL-5 monoclonal antibodies for atopic dermatitis, eosinophilic esophagitis, and asthma yielded mixed to negative results (Leckie et al., 2000; Oldhoff et al., 2005; Flood-Page et al., 2007). Although some of these findings may have reflected patient selection (Haldar et al., 2009; Bel et al., 2014; Ortega et al., 2014), these trials have not revealed a clear pathological role for eosinophils in allergic disease. Pathological findings from lesional skin of patients with atopic dermatitis are characterized by the presence of eosinophils, basophils, and VCAM-1$^+$ endothelium (Wakita et al., 1994; Ito et al., 2011), as seen in the models used here. Moreover, in allergic individuals with dust mite–specific IgE, dust mite antigen applied to unaffected skin resulted in the formation of an eczematous lesion within 2–3 d, characterized by perivascular basophil and eosinophil infiltration (Mitchell et al., 1982). Targeting the IL-4–IL-13 pathway using an IL-4Rα antagonist was efficacious in the treatment of patients with moderate to severe atopic dermatitis (Beck et al., 2014), confirming the clinical relevance of this pathway, although further study will be needed to dissect the mechanisms involved.

Our data reveal a means by which a recruited cell can alter its migratory kinetics based on recognition of specific local signals. Transendothelial migration of leukocytes consists of a multistep process that includes (a) selectin-mediated rolling, (b) integrin-mediated firm adhesion, (c) intravascular crawling to sites amenable for diapedesis, and (d) endothelial transmigration (Kolaczkowska and Kubes, 2013). Although basophils follow canonical pathways of rolling and firm adhesion (Saeki et al., 2013; unpublished data), the enhanced interactions at the endothelial interface after IgE activation suggest unique antigen-dependent regulation of the last two steps. Our data support a model in which activation during diapedesis alters basophil motility and promotes the "arrest" of basophils within or along the endothelial basement membrane where antigen might be encountered. This change in transmigration is in part dependent on signaling through the FAKs activated during integrin and FcεRI coengagement.

The focal adhesion kinases FAK and Pyk2 are activated by cell surface receptors in response to diverse stimuli, including extracellular matrix constituents, integrin ligation, growth factors, antigen receptor clustering, and chemokines (Mitra et al., 2005). During integrin-mediated activation, FAK/Pyk2 does not directly bind the cytoplasmic tails of integrins in vivo. Instead, FAK/Pyk2 interacts with the proteins paxillin and talin, which in turn link integrins to the actin cytoskeleton. Most studies suggest that inhibition or loss of FAK leads to loss of migration (Mitra et al., 2005), and we observed a similar loss of basophil migration with or without antigen at high concentrations of inhibitor (unpublished data). These data suggest that basophil adherence to endothelium can be "tuned" by concomitant engagement of FcεRI and integrins. Although several models could account for this, our data could be consistent with impaired degranulation as the absence of FAK leads to impaired mast cell degranulation (Vial et al., 2000). This would abrogate the subsequent release or cell surface display of molecules that could promote adhesion to endothelial cells (Kannan et al., 1996). These kinases may have a more general role in myeloid cell degranulation as neutrophils lacking Pyk2 also show defective degranulation (Kamen et al., 2011).

The lack of a prominent mast cell contribution is intriguing because mast cells release an array of vasoactive substances and cytokines after IgE-mediated activation (Galli and Tsai, 2010). As shown here, and as corroborated in other models of cutaneous hypersensitivity (Mukai et al., 2005), we found no effects on eosinophil or Gr-1$^+$ infiltrates in mast cell–deficient mice (Fig. 1 E

Downloaded from jem.rupress.org on March 21, 2015

and not depicted). This and prior data support nonredundant contributions of mast cells and basophils during allergic immune responses, with activated mast cells exerting primary effects on vascular permeability that enhance the influx of serum proteins into the tissue space (Medzhitov, 2008). Basophils might additionally amplify these effects through release of mMCP-11 (Yamagishi et al., 2011). In humans (but not mice), eosinophils have been suggested to express the trimeric form of FcεRI ($\alpha\gamma_2$; Gould and Sutton, 2008), but the functional relevance of this in the context of allergic dermatitis remains indeterminate.

Our reporter data and genetic evidence indicate a prominent role for basophil-derived IL-4 in regulating eosinophilic dermatitis. However, the basophil-specific knockouts exhibited a more modest decrease in eosinophil accumulation as compared with either basophil-deficient mice or global IL-4 knockouts. Although incomplete recombination (estimated at 60–75% efficiency) of the 4/13 locus could be responsible, additional basophil-derived factors could also contribute. Activated basophils have been reported to produce TNF (Sokol et al., 2008), which can also promote VCAM-1 up-regulation (Neumann et al., 1996). The relative decrease in eosinophil influx in mice receiving intradermal IL-4 compared with the IgE-mediated response may reflect such contributions. Additionally, although endothelial cells express the type II IL-4R, our data do not formally rule out an intermediate cell type that responds to IL-4 and thus indirectly promotes endothelial cell VCAM-1 expression.

Although many details of the molecular and cellular circuitry governing specification of immune responses have been defined, our data reveal a novel paradigm by which rare circulating basophils can alter their migratory behavior in response to tissue-derived antigens and thereby change the characteristics of the localized inflammatory response through modulation of endothelial ligands. Our data provide a link between eosinophils and IgE through an interaction of antigen-activated basophils and the endothelium, which facilitates prolonged delivery of basophil IL-4 to the endothelium to modulate endothelial adhesins. The identification of basophils as "gatekeepers" for allergic skin diseases could provide new strategies to control allergic disease by interdicting this central pathway for eosinophil accumulation in skin, and perhaps in other tissues.

MATERIALS AND METHODS

Mice. Basoph8, KN2, IL-4/13^{flox}, 4get, and Rosa-DTA have been previously described (Mohrs et al., 2001, 2005; Voehringer et al., 2008, 2009). C57BL/6 mice were obtained from The Jackson Laboratory. Rag2$^{-/-}$ mice were obtained from Taconic. MCPT5-cre BAC transgenic (provided by A. Roers, University of Technology Dresden, Dresden, Germany), *Alox5*$^{-/-}$, *Ltb4r1*$^{-/-}$, and *Fcer1a*$^{-/-}$ mice have been described previously (Dombrowicz et al., 1993; Chen et al., 1994; Tager et al., 2000; Scholten et al., 2008). All mice were backcrossed to C57BL/6 for at least 10 generations, except for experiments with Basoph8 × IL4/13^{flox} mice, which were BALB/c × C57BL/6 F1 mice. Mice were housed in specific pathogen–free facilities. Animal use was governed and approved by the University of California, San Francisco (UCSF) Institutional Animal Care and Use Committee.

IgE dermatitis and tissue preparation. Mice were injected via the tail vein with 2 µg DNP-specific monoclonal IgE, Spe-7 (Sigma-Aldrich). 24–36 h later, mice were challenged with a solution of 0.6% DNFB diluted in a 1:1 mixture of acetone and dibutylphthalate applied onto the dorsal and ventral halves of the ear (Matsuda et al., 2010). 10 µl of solution was placed on each side of the ear. At designated times, ears were dissected, separated into ventral and dorsal halves, and finely minced. Tissue was resuspended in HBSS plus 1 Wünsch U/ml Liberase TL (Roche) for 45 min at 37°C with constant agitation. Digestion was quenched with a 3-vol excess of ice-cold PBS with 3% fetal bovine serum and strained through a 70-µm mesh before analysis. For control IgE experiments, anti-OVA (E-G5; Chondrex) was used in place of Spe-7.

Antibodies, cell populations, and flow cytometry. Antibodies against the following antigens were used: CD11b (M1/70; eBioscience), CD49b (DX5; eBioscience), Siglec-F (E50-2440; BD), Ly6G/C (RB6-8C5; BD), FcεRI (Mar-1; BioLegend), CD45 (30-F11; BioLegend), CD34 (RAM34; eBioscience), ESAM-1 (1G8; BioLegend), CD31 (390; eBioscience), c-kit (2B7; BioLegend), CD106 (429; eBioscience), IL-4Rα (mIL4-M1; BD), and CD213a1 (13MOKA; eBioscience). Key cell populations were defined as follows: (a) eosinophils, FSC^{lo}SSC^{hi}CD11b^{+}Siglec-F^{+} or FSC^{lo}SSC^{hi}Siglec-F^{+}4get^{+}; (b) basophils, FSC^{lo}SSC^{lo}CD49b^{+}FcεRI^{+}Gr-1^{-}CD4^{-}CD8^{-}CD19^{-}γδ^{-}Siglec-F^{-} or FSC^{lo}SSC^{lo}Basoph8^{+}CD49b^{+}; (c) mast cells, 4get^{+}ckit^{+} or FSC^{hi}SSC^{hi}c-kit^{+} CD11a^{-}CD44^{+}; (d) endothelial cells, CD45^{-}CD34^{+}ESAM-1^{+}; and (e) PMNs/monocytes, Gr-1^{+}CD11b^{+}. Flow cytometry data acquisition was performed on an LSRII (BD), using FlowJo to analyze the data.

Immunization. 100 µl of a 0.5 mg/ml solution of DNP-OVA (Biosearch Technologies) was mixed dropwise with agitation with Imject Alum (Thermo Fisher Scientific) at a 1:1 ratio. The solution was then mixed for 30 min and injected into the peritoneum of index mice.

Epicutaneous antigen application. Mice received 2 µg anti-TNP IgE (C38-2; BD) i.v. 1 d before challenge. For the challenge, mice were anesthetized and then gently tape stripped (six times on the dorsal surface of the ear and six times on the ventral surface) using Scotch Tape (3M). A 1 × 1–cm piece of gauze was then soaked with 50 µl of a 1 µg/µl solution of TNP-OVA in PBS. The gauze was then affixed to each side of the ear for 1 h using a DuoDERM patch (ConvaTec) as a dressing. The patch was then removed, and the mice were analyzed at the indicated time.

In vivo antibody infusions. For labeling the vasculature in situ, 4 µg anti–CD31-APC (clone 390; eBioscience) was administered i.v. 10 min before analysis. For VCAM-1 experiments, 2 µg anti–VCAM-1 antibody (clone 429; eBioscience) was administered i.v. 10 min before analysis.

Whole mount microscopy. After dissection, the ears were split into dorsal and ventral halves, immobilized in a Petri dish dermal side up, and submerged in ice-cold PBS. Samples were analyzed using a confocal microscope (A1r; Nikon) using a 25× objective (NA = 1.05) or a 20× objective (NA = 0.95). Imaging volumes were analyzed using Imaris software (Bitmap). VCAM-1 segmentation was performed by identifying the borders of the VCAM-1 patches along the long axis of the vessel and then segmenting the vessel based on these borders. 11 z-stacks with a total length of ~10 mm of vessels were analyzed. In total, these z-stacks contained ~0.1 µm^3 of VCAM-1^{+} segments and 0.08 µm^3 VCAM-1^{-} segments that were assessed.

Immunofluorescence microscopy. Intact ears were fixed in a 4% paraformaldehyde solution in PBS for 2 h on ice, rinsed with PBS overnight, and then incubated in 30% sucrose for 2 h. Ears were embedded in OCT (Sakura) and cut into 8-µm sections. Sections were stained with anti–Siglec-F biotin and detected with streptavidin Alexa Flour 555. DAPI was used as a counterstain. Images were acquired using an Axio Imager 2 microscope using a 20× objective with NA = 0.80 and analyzed using AxioVision software (both Carl Zeiss).

Antibody blockade. 100 µg antagonist antibodies for α4 integrin (PS/2; provided by J. Cyster, UCSF) was administered via intraperitoneal injection 3 h before challenge. Isotype control antibodies were administered in control mice.

Transwell migration assays. To generate a sufficient source of basophils for the assay, we administered IL-3 complexes (10 µg IL-3 [R&D Systems]

Downloaded from jem.rupress.org on March 21, 2015

complexed to 50 μg anti–IL-3 [MP2-8F8; BioLegend] for 5 min at room temperature) to Basoph8 mice 3 d before migration assays (Finkelman et al., 1993). Mice were then sensitized with 5 μg monoclonal IgE against TNP (C38-2; BD) 24 h before the assay. On the day of the migration assay, splenocytes were enumerated, and a total of 12,500 basophils were placed in the upper chamber of the transwell apparatus with LTB4 at 5 nM ± 100 ng/ml TNP-OVA (Biosearch Technologies) placed in the lower chamber analogous to published protocols (Ansel et al., 1999). For transendothelial migration assays, 1.5×10^5 bEnd.3 cells (an immortalized, mouse brain endothelial cell line) were placed on gelatinized transwell inserts 40 h before the assay (Montesano et al., 1990). Basophils in the lower chamber were assessed by flow cytometry after a 4-h incubation at 37°C. Each condition was performed in duplicate. Inhibitors PF 431396 and PF 573228 (Tocris Bioscience) were diluted to the indicated concentration and placed in both the upper and lower wells of the transwell just before addition of the basophils.

Statistical analysis. One-way ANOVA was used for all in vivo analyses involving three or more groups. Intergroup analyses were then performed using Tukey's multiple comparisons test. For analyses with only two groups, a two-tailed, unpaired Student's *t* test was performed. On all graphs, p-values are denoted by the following nomenclature: *, $P < 0.05$; **, $P < 0.01$; ***, $P < 0.001$; ****, $P < 0.0001$. All analyses were performed using Prism software version 6.0b (GraphPad Software).

Online supplemental material. The gating scheme for flow cytometry of basophil, eosinophils, and neutrophils is contained in Fig. S1. Online supplemental material is available at http://www.jem.org/cgi/content/full/jem.20141671/DC1.

We thank J. Cyster and A. Roers for reagents, M. Krummel for assistance with imaging experiments, S. Rosen and C. Lowell for scientific discussions and review of the manuscript, and Z. Wang for technical assistance.

This work was supported by the A.P. Giannini Medical Research Foundation (to L.E. Cheng); National Institutes of Health grants AI095319 (to L.E. Cheng), AI103146 (to C.D.C. Allen), AI026918 (R.M. Locksley), AI030663 (R.M. Locksley), and AI119944 (R.M. Locksley); the Howard Hughes Medical Institute (to R.M. Locksley); and the University of California, San Francisco Sabre Center (to L.E. Cheng, C.D.C. Allen, and R.M. Locksley).

The authors declare no competing financial interests.

Submitted: 29 August 2014
Accepted: 11 February 2015

REFERENCES

Ansel, K.M., L.J. McHeyzer-Williams, V.N. Ngo, M.G. McHeyzer-Williams, and J.G. Cyster. 1999. In vivo–activated CD4 T cells upregulate CXC chemokine receptor 5 and reprogram their response to lymphoid chemokines. *J. Exp. Med.* 190:1123–1134. http://dx.doi.org/10.1084/jem.190.8.1123

Askenase, P.W. 1979. Mechanisms of hypersensitivity: cellular interactions. Basophil arrival and function in tissue hypersensitivity reactions. *J. Allergy Clin. Immunol.* 64:79–89. http://dx.doi.org/10.1016/0091-6749(79)90041-1

Baumhueter, S., N. Dybdal, C. Kyle, and L.A. Lasky. 1994. Global vascular expression of murine CD34, a sialomucin-like endothelial ligand for L-selectin. *Blood.* 84:2554–2565.

Beck, L.A., D. Thaçi, J.D. Hamilton, N.M. Graham, T. Bieber, R. Rocklin, J.E. Ming, H. Ren, R. Kao, E. Simpson, et al. 2014. Dupilumab treatment in adults with moderate-to-severe atopic dermatitis. *N. Engl. J. Med.* 371:130–139. http://dx.doi.org/10.1056/NEJMoa1314768

Bel, E.H., S.E. Wenzel, P.J. Thompson, C.M. Prazma, O.N. Keene, S.W. Yancey, H.G. Ortega, and I.D. Pavord; SIRIUS Investigators. 2014. Oral glucocorticoid-sparing effect of mepolizumab in eosinophilic asthma. *N. Engl. J. Med.* 371:1189–1197. http://dx.doi.org/10.1056/NEJMoa1403291

Boguniewicz, M., and D.Y. Leung. 2010. Recent insights into atopic dermatitis and implications for management of infectious complications. *J. Allergy Clin. Immunol.* 125:4–13. http://dx.doi.org/10.1016/j.jaci.2009.11.027

Chan, L.S., N. Robinson, and L. Xu. 2001. Expression of interleukin-4 in the epidermis of transgenic mice results in a pruritic inflammatory skin disease: an experimental animal model to study atopic dermatitis. *J. Invest. Dermatol.* 117:977–983. http://dx.doi.org/10.1046/j.0022-202x.2001.01484.x

Chen, X.S., J.R. Sheller, E.N. Johnson, and C.D. Funk. 1994. Role of leukotrienes revealed by targeted disruption of the 5-lipoxygenase gene. *Nature.* 372:179–182. http://dx.doi.org/10.1038/372179a0

Cheng, L.E., Z.E. Wang, and R.M. Locksley. 2010. Murine B cells regulate serum IgE levels in a CD23-dependent manner. *J. Immunol.* 185:5040–5047. http://dx.doi.org/10.4049/jimmunol.1001900

Cheng, L.E., K. Hartmann, A. Roers, M.F. Krummel, and R.M. Locksley. 2013. Perivascular mast cells dynamically probe cutaneous blood vessels to capture immunoglobulin E. *Immunity.* 38:166–175. http://dx.doi.org/10.1016/j.immuni.2012.09.022

Dombrowicz, D., V. Flamand, K.K. Brigman, B.H. Koller, and J.P. Kinet. 1993. Abolition of anaphylaxis by targeted disruption of the high affinity immunoglobulin E receptor alpha chain gene. *Cell.* 75:969–976. http://dx.doi.org/10.1016/0092-8674(93)90540-7

Egawa, M., K. Mukai, S. Yoshikawa, M. Iki, N. Mukaida, Y. Kawano, Y. Minegishi, and H. Karasuyama. 2013. Inflammatory monocytes recruited to allergic skin acquire an anti-inflammatory M2 phenotype via basophil-derived interleukin-4. *Immunity.* 38:570–580. http://dx.doi.org/10.1016/j.immuni.2012.11.014

Finkelman, F.D., K.B. Madden, S.C. Morris, J.M. Holmes, N. Boiani, I.M. Katona, and C.R. Maliszewski. 1993. Anti-cytokine antibodies as carrier proteins. Prolongation of in vivo effects of exogenous cytokines by injection of cytokine-anti-cytokine antibody complexes. *J. Immunol.* 151:1235–1244.

Flood-Page, P., C. Swenson, I. Faiferman, J. Matthews, M. Williams, L. Brannick, D. Robinson, S. Wenzel, W. Busse, T.T. Hansel, and N.C. Barnes; International Mepolizumab Study Group. 2007. A study to evaluate safety and efficacy of mepolizumab in patients with moderate persistent asthma. *Am. J. Respir. Crit. Care Med.* 176:1062–1071. http://dx.doi.org/10.1164/rccm.200701-085OC

Galli, S.J., and M. Tsai. 2010. Mast cells in allergy and infection: versatile effector and regulatory cells in innate and adaptive immunity. *Eur. J. Immunol.* 40:1843–1851. http://dx.doi.org/10.1002/eji.201040559

Gessner, A., K. Mohrs, and M. Mohrs. 2005. Mast cells, basophils, and eosinophils acquire constitutive IL-4 and IL-13 transcripts during lineage differentiation that are sufficient for rapid cytokine production. *J. Immunol.* 174:1063–1072. http://dx.doi.org/10.4049/jimmunol.174.2.1063

Gould, H.J., and B.J. Sutton. 2008. IgE in allergy and asthma today. *Nat. Rev. Immunol.* 8:205–217. http://dx.doi.org/10.1038/nri2273

Haldar, P., C.E. Brightling, B. Hargadon, S. Gupta, W. Monteiro, A. Sousa, R.P. Marshall, P. Bradding, R.H. Green, A.J. Wardlaw, and I.D. Pavord. 2009. Mepolizumab and exacerbations of refractory eosinophilic asthma. *N. Engl. J. Med.* 360:973–984. http://dx.doi.org/10.1056/NEJMoa0808991

Hirata, K.-i., T. Ishida, K. Penta, M. Rezaee, E. Yang, J. Wohlgemuth, and T. Quertermous. 2001. Cloning of an immunoglobulin family adhesion molecule selectively expressed by endothelial cells. *J. Biol. Chem.* 276:16223–16231. http://dx.doi.org/10.1074/jbc.M100630200

Ito, Y., T. Satoh, K. Takayama, C. Miyagishi, A.F. Walls, and H. Yokozeki. 2011. Basophil recruitment and activation in inflammatory skin diseases. *Allergy.* 66:1107–1113. http://dx.doi.org/10.1111/j.1398-9995.2011.02570.x

Jin, G., T. Matsushita, Y. Hamaguchi, D. Le Huu, T. Ishii, M. Hasegawa, K. Obata, H. Karasuyama, K. Takehara, and M. Fujimoto. 2012. Basophils and mast cells play critical roles for leukocyte recruitment in IgE-mediated cutaneous reverse passive Arthus reaction. *J. Dermatol. Sci.* 67:181–189. http://dx.doi.org/10.1016/j.jdermsci.2012.06.005

Kamen, L.A., J. Schlessinger, and C.A. Lowell. 2011. Pyk2 is required for neutrophil degranulation and host defense responses to bacterial infection. *J. Immunol.* 186:1656–1665. http://dx.doi.org/10.4049/jimmunol.1002093

Kannan, K., R.M. Stewart, W. Bounds, S.R. Carlsson, M. Fukuda, K.W. Betzing, and R.F. Holcombe. 1996. Lysosome-associated membrane proteins h-LAMP1 (CD107a) and h-LAMP2 (CD107b) are activation-dependent cell surface glycoproteins in human peripheral blood mononuclear

Downloaded from jem.rupress.org on March 21, 2015

cells which mediate cell adhesion to vascular endothelium. *Cell. Immunol.* 171:10–19. http://dx.doi.org/10.1006/cimm.1996.0167

Kolaczkowska, E., and P. Kubes. 2013. Neutrophil recruitment and function in health and inflammation. *Nat. Rev. Immunol.* 13:159–175. http://dx.doi.org/10.1038/nri3399

Leckie, M.J., A. ten Brinke, J. Khan, Z. Diamant, B.J. O'Connor, C.M. Walls, A.K. Mathur, H.C. Cowley, K.F. Chung, R. Djukanovic, et al. 2000. Effects of an interleukin-5 blocking monoclonal antibody on eosinophils, airway hyper-responsiveness, and the late asthmatic response. *Lancet.* 356:2144–2148. http://dx.doi.org/10.1016/S0140-6736(00)03496-6

Liu, F.T., H. Goodarzi, and H.Y. Chen. 2011. IgE, mast cells, and eosinophils in atopic dermatitis. *Clin. Rev. Allergy Immunol.* 41:298–310. http://dx.doi.org/10.1007/s12016-011-8252-4

Matsuda, T., T. Maruyama, H. Iizuka, A. Kondo, T. Tamai, K. Kurohane, and Y. Imai. 2010. Phthalate esters reveal skin-sensitizing activity of phenethyl isothiocyanate in mice. *Food Chem. Toxicol.* 48:1704–1708. http://dx.doi.org/10.1016/j.fct.2010.03.049

Matsuoka, K., H. Shitara, C. Taya, K. Kohno, Y. Kikkawa, and H. Yonekawa. 2013. Novel basophil- or eosinophil-depleted mouse models for functional analyses of allergic inflammation. *PLoS ONE.* 8:e60958. http://dx.doi.org/10.1371/journal.pone.0060958

Medzhitov, R. 2008. Origin and physiological roles of inflammation. *Nature.* 454:428–435. http://dx.doi.org/10.1038/nature07201

Mitchell, E.B., J. Crow, M.D. Chapman, S.S. Jouhal, F.M. Pope, and T.A. Platts-Mills. 1982. Basophils in allergen-induced patch test sites in atopic dermatitis. *Lancet.* 1:127–130. http://dx.doi.org/10.1016/S0140-6736(82)90379-8

Mitra, S.K., D.A. Hanson, and D.D. Schlaepfer. 2005. Focal adhesion kinase: in command and control of cell motility. *Nat. Rev. Mol. Cell Biol.* 6:56–68. http://dx.doi.org/10.1038/nrm1549

Miyake, K., I.L. Weissman, J.S. Greenberger, and P.W. Kincade. 1991. Evidence for a role of the integrin VLA-4 in lympho-hemopoiesis. *J. Exp. Med.* 173:599–607. http://dx.doi.org/10.1084/jem.173.3.599

Mohrs, K., A.E. Wakil, N. Killeen, R.M. Locksley, and M. Mohrs. 2005. A two-step process for cytokine production revealed by IL-4 dual-reporter mice. *Immunity.* 23:419–429. http://dx.doi.org/10.1016/j.immuni.2005.09.006

Mohrs, M., K. Shinkai, K. Mohrs, and R.M. Locksley. 2001. Analysis of type 2 immunity in vivo with a bicistronic IL-4 reporter. *Immunity.* 15:303–311. http://dx.doi.org/10.1016/S1074-7613(01)00186-8

Montesano, R., M.S. Pepper, U. Möhle-Steinlein, W. Risau, E.F. Wagner, and L. Orci. 1990. Increased proteolytic activity is responsible for the aberrant morphogenetic behavior of endothelial cells expressing the middle T oncogene. *Cell.* 62:435–445. http://dx.doi.org/10.1016/0092-8674(90)90009-4

Mukai, K., K. Matsuoka, C. Taya, H. Suzuki, H. Yokozeki, K. Nishioka, K. Hirokawa, M. Etori, M. Yamashita, T. Kubota, et al. 2005. Basophils play a critical role in the development of IgE-mediated chronic allergic inflammation independently of T cells and mast cells. *Immunity.* 23:191–202. http://dx.doi.org/10.1016/j.immuni.2005.06.011

Neumann, B., T. Machleidt, A. Lifka, K. Pfeffer, D. Vestweber, T.W. Mak, B. Holzmann, and M. Krönke. 1996. Crucial role of 55-kilodalton TNF receptor in TNF-induced adhesion molecule expression and leukocyte organ infiltration. *J. Immunol.* 156:1587–1593.

Ohnmacht, C., C. Schwartz, M. Panzer, I. Schiedewitz, R. Naumann, and D. Voehringer. 2010. Basophils orchestrate chronic allergic dermatitis and protective immunity against helminths. *Immunity.* 33:364–374. http://dx.doi.org/10.1016/j.immuni.2010.08.011

Oldhoff, J.M., U. Darsow, T. Werfel, K. Katzer, A. Wulf, J. Laifaoui, D.J. Hijnen, S. Plötz, E.F. Knol, A. Kapp, et al. 2005. Anti-IL-5 recombinant humanized monoclonal antibody (mepolizumab) for the treatment of atopic dermatitis. *Allergy.* 60:693–696. http://dx.doi.org/10.1111/j.1398-9995.2005.00791.x

Ortega, H.G., M.C. Liu, I.D. Pavord, G.G. Brusselle, J.M. FitzGerald, A. Chetta, M. Humbert, L.E. Katz, O.N. Keene, S.W. Yancey, and P. Chanez; MENSA Investigators. 2014. Mepolizumab treatment in patients with severe eosinophilic asthma. *N. Engl. J. Med.* 371:1198–1207. http://dx.doi.org/10.1056/NEJMoa1403290

Oyoshi, M.K., R.P. Larson, S.F. Ziegler, and R.S. Geha. 2010. Mechanical injury polarizes skin dendritic cells to elicit a T_H2 response by inducing cutaneous thymic stromal lymphopoietin expression. *J. Allergy Clin. Immunol.* 126:976–984. http://dx.doi.org/10.1016/j.jaci.2010.08.041

Qi, X., J. Hong, L. Chaves, Y. Zhuang, Y. Chen, D. Wang, J. Chabon, B. Graham, K. Ohmori, Y. Li, and H. Huang. 2013. Antagonistic regulation by the transcription factors C/EBPα and MITF specifies basophil and mast cell fates. *Immunity.* 39:97–110. http://dx.doi.org/10.1016/j.immuni.2013.06.012

Reese, T.A., H.E. Liang, A.M. Tager, A.D. Luster, N. Van Rooijen, D. Voehringer, and R.M. Locksley. 2007. Chitin induces accumulation in tissue of innate immune cells associated with allergy. *Nature.* 447:92–96. http://dx.doi.org/10.1038/nature05746

Saeki, K., T. Satoh, and H. Yokozeki. 2013. α(1,3) Fucosyltransferases IV and VII are essential for the initial recruitment of basophils in chronic allergic inflammation. *J. Invest. Dermatol.* 133:2161–2169. http://dx.doi.org/10.1038/jid.2013.160

Scholten, J., K. Hartmann, A. Gerbaulet, T. Krieg, W. Müller, G. Testa, and A. Roers. 2008. Mast cell-specific Cre/loxP-mediated recombination in vivo. *Transgenic Res.* 17:307–315. http://dx.doi.org/10.1007/s11248-007-9153-4

Simon, D., L.R. Braathen, and H.U. Simon. 2004. Eosinophils and atopic dermatitis. *Allergy.* 59:561–570. http://dx.doi.org/10.1111/j.1398-9995.2004.00476.x

Sokol, C.L., G.M. Barton, A.G. Farr, and R. Medzhitov. 2008. A mechanism for the initiation of allergen-induced T helper type 2 responses. *Nat. Immunol.* 9:310–318. http://dx.doi.org/10.1038/ni1558

Sullivan, B.M., H.E. Liang, J.K. Bando, D. Wu, L.E. Cheng, J.K. McKerrow, C.D. Allen, and R.M. Locksley. 2011. Genetic analysis of basophil function in vivo. *Nat. Immunol.* 12:527–535. http://dx.doi.org/10.1038/ni.2036

Tager, A.M., J.H. Dufour, K. Goodarzi, S.D. Bercury, U.H. von Andrian, and A.D. Luster. 2000. BLTR mediates leukotriene B_4–induced chemotaxis and adhesion and plays a dominant role in eosinophil accumulation in a murine model of peritonitis. *J. Exp. Med.* 192:439–446. http://dx.doi.org/10.1084/jem.192.3.439

Tozawa, H., Y. Kanki, J. Suehiro, S. Tsutsumi, T. Kohro, Y. Wada, H. Aburatani, W.C. Aird, T. Kodama, and T. Minami. 2011. Genome-wide approaches reveal functional interleukin-4-inducible STAT6 binding to the vascular cell adhesion molecule 1 promoter. *Mol. Cell. Biol.* 31:2196–2209. http://dx.doi.org/10.1128/MCB.01430-10

Vial, D., H. Okazaki, and R.P. Siraganian. 2000. The NH2-terminal region of focal adhesion kinase reconstitutes high affinity IgE receptor-induced secretion in mast cells. *J. Biol. Chem.* 275:28269–28275.

Voehringer, D., K. Shinkai, and R.M. Locksley. 2004. Type 2 immunity reflects orchestrated recruitment of cells committed to IL-4 production. *Immunity.* 20:267–277. http://dx.doi.org/10.1016/S1074-7613(04)00026-3

Voehringer, D., H.E. Liang, and R.M. Locksley. 2008. Homeostasis and effector function of lymphopenia-induced "memory-like" T cells in constitutively T cell-depleted mice. *J. Immunol.* 180:4742–4753. http://dx.doi.org/10.4049/jimmunol.180.7.4742

Voehringer, D., D. Wu, H.E. Liang, and R.M. Locksley. 2009. Efficient generation of long-distance conditional alleles using recombineering and a dual selection strategy in replicate plates. *BMC Biotechnol.* 9:69. http://dx.doi.org/10.1186/1472-6750-9-69

Wakita, H., T. Sakamoto, Y. Tokura, and M. Takigawa. 1994. E-selectin and vascular cell adhesion molecule-1 as critical adhesion molecules for infiltration of T lymphocytes and eosinophils in atopic dermatitis. *J. Cutan. Pathol.* 21:33–39. http://dx.doi.org/10.1111/j.1600-0560.1994.tb00688.x

Woodfin, A., M.B. Voisin, M. Beyrau, B. Colom, D. Caille, F.M. Diapouli, G.B. Nash, T. Chavakis, S.M. Albelda, G.E. Rainger, et al. 2011. The junctional adhesion molecule JAM-C regulates polarized transendothelial migration of neutrophils in vivo. *Nat. Immunol.* 12:761–769. http://dx.doi.org/10.1038/ni.2062

Woodruff, P.G., B. Modrek, D.F. Choy, G. Jia, A.R. Abbas, A. Ellwanger, L.L. Koth, J.R. Arron, and J.V. Fahy. 2009. T-helper type 2–driven inflammation defines major subphenotypes of asthma. *Am. J. Respir. Crit. Care Med.* 180:388–395. http://dx.doi.org/10.1164/rccm.200903-0392OC

Yamagishi, H., Y. Mochizuki, T. Hamakubo, K. Obata, T. Ugajin, S. Sato, Y. Kawano, Y. Minegishi, and H. Karasuyama. 2011. Basophil-derived mouse mast cell protease 11 induces microvascular leakage and tissue edema in a mast cell-independent manner. *Biochem. Biophys. Res. Commun.* 415:709–713. http://dx.doi.org/10.1016/j.bbrc.2011.10.150

Downloaded from jem.rupress.org on March 21, 2015

The Journal of Experimental Medicine

SUPPLEMENTAL MATERIAL

Cheng et al., http://www.jem.org/cgi/content/full/jem.20141671/DC1

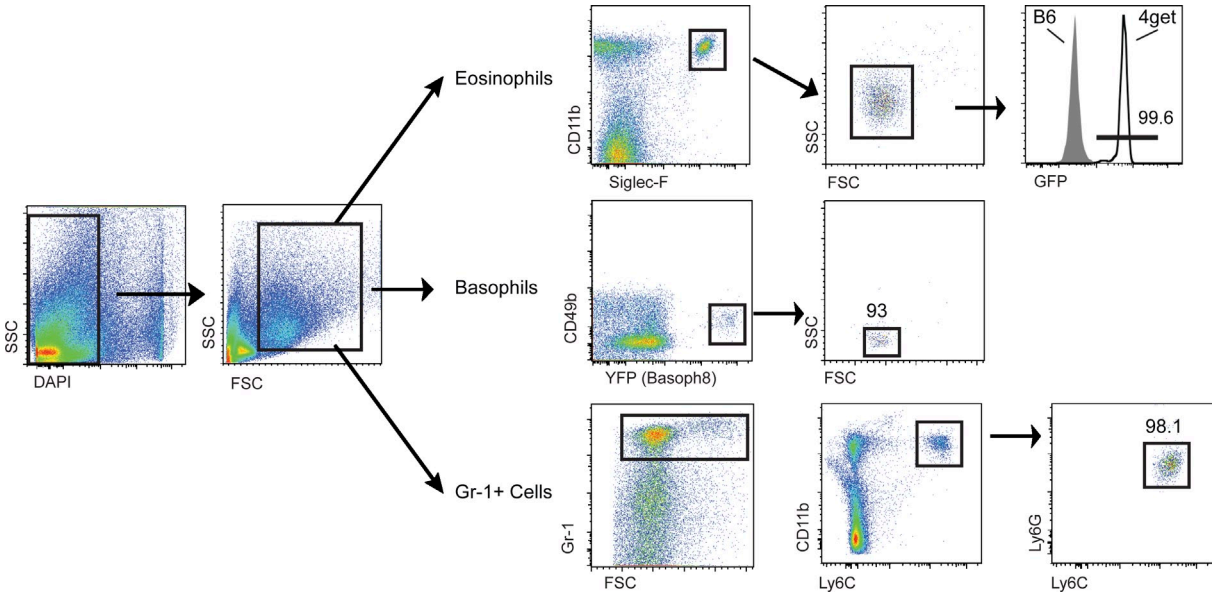

Figure S1. Gating scheme for eosinophils ($FSC^{lo}SSC^{hi}CD11b^{+}Siglec\text{-}F^{+}$), basophils ($FSC^{lo}SSC^{lo}CD49b^{+}YFP^{+}$), and Gr-1^{+} cells on day 3 after challenge. For eosinophils, the histograms at the right reveals uniform expression of GFP of Siglec-F^{+}CD11b^{+}FSC^{lo}SSC^{hi} cells when derived from *4get* mice (Mohrs et al., 2001). For Gr-1^{+} cells, parallel examination of ear suspensions revealed that most all of these cells were neutrophils because Ly6C^{+} cells were also Ly6G^{+}.

REFERENCE

Mohrs, M., K. Shinkai, K. Mohrs, and R.M. Locksley. 2001. Analysis of type 2 immunity in vivo with a bicistronic IL-4 reporter. *Immunity*. 15:303–311. http://dx.doi.org/10.1016/S1074-7613(01)00186-8